Original Paper

Cellular Physiology and Biochemistry

Cell Physiol Biochem 2008;21:225-238

Accepted: September 27, 2007

Selenium Attenuates ROS-Mediated Apoptotic Cell Death of Injured Spinal Cord through Prevention of Mitochondria Dysfunction; *in Vitro* and *in Vivo* Study

Jee Eun Yeo, Jeong Hwan Kim and Soo Kyung Kang

Department of Physiology, College of Medicine, Pusan National University, Busan

Key Words

Apoptotic Cell Death Function Recovery • Inflammation • Myelination • Neuroprotection • Selenium • Spinal Cord Injury

Abstract

The primary objective of this study was to determine the possible apoptotic cell death preventive effects of the antioxidant selenium using an experimental rat spinal cord injury (SCI) model and cultured spinal cord-derived neural progenitor cells (NPCs). Sodium selenite treatment exerted a profound preventive effect on apoptotic cell death, including p-P38, p-SAPK/JNK, caspases, and PARP activity, and ameliorated astrogliosis and hypomyelination, which occurs in regions of active cell death in the spinal cords of SCI rats. The foremost protective effect of selenite in SCI would therefore be manifested in the suppression of acute secondary apoptotic cell death. However, selenite does not appear to exert an anti-inflammatory function associated with active microglia and macrophage propagation or infiltration into the lesion site. Selenite-mediated neuroprotection has been linked to selenite's attenuation or inhibition of p38 mitogen-activated protein kinase, pSAPK/JNK, and Bax activation in *in vitro* and *in vivo* SCI lesion sites. Selenite also attenuated cell death via the prevention of cytochrome c release, caspase activation, and ROS accumulation in the cytosol. Also, our study showed that selenite administered immediately after SCI significantly diminishes functional deficits. The selenite-treated group recovered hind limb reflexes more rapidly, and a higher percentage of these rats regained responses to a greater degree than was seen in the untreated injured rats. Our data indicate that the therapeutic outcome of selenite is most likely the consequence of its comprehensive apoptotic cell death blocking effects, resulting in the protection of white matter, oligodendrocytes, and neurons, and the inhibition of astrogliosis. The finding that the administration of selenite prevents secondary pathological events in traumatic spinal cord injuries, and promotes the recovery of motor function in an animal model. Its efficacy may facilitate the development of novel drug targets for the treatment of SCI.

Introduction

Traumatic spinal cord injury (SCI) induces permanent neurological deficits resulting from the loss of spinal cord

KARGER

Fax +41 61 306 12 34
E-Mail karger@karger.ch
www.karger.com

1015-8987/08/0213-0225$24.50/0

Accessible online at:
www.karger.com/cpb

Prof. Soo Kyung Kang
Department of Physiology
College of Medicine, Pusan National University
Busan, 602-739 (South Korea)
E-Mail skkang@pusan.ac.kr

neurons and axons. Landmark experiments conducted more than 20 years ago showed that neurologic deficits are not attributable to an intrinsic inability of central nervous system (CNS) neurons to regenerate, but rather to unfavorable CNS environments [1]. The devastating neurological consequences of spinal cord injury in adults are attributed principally to retrograde neuronal cell death and the failure of surviving neurons to regenerate their severed axons. The principal autodestructive processes that have been thus far postulated are secondary ischemic changes, and free radical induced-lipid peroxidation which damages the lipid membranes in the spinal cord. All of these processes are believed to induce autodestructive damage to the spinal cord; they are triggered by the mechanisms of initial spinal cord injury, but the detailed biocascades inherent to this process remain incompletely understood [2, 3].

Oxidative injury has been causally linked to a variety of neurodegenerative diseases, including Alzheimer's disease [4], Parkinson's disease [5], amyotrophic lateral sclerosis [6], spinal cord injury, and conditions including ischemia and excitotoxicity. Oxidative damage is mediated by reactive oxygen species (ROS), which can be generated after cell lysis, oxidative burst (as part of the immune response) [7, 8], or the presence of an excess of free transition metals (which can function catalytically to generate free radicals) [9]. ROS can also be generated as a byproduct of normal cellular respiration, which is associated principally with mitochondrial electron transport [10]. Cellular defense mechanisms against oxidative damage include the enzymatic conversion of ROS to less reactive species, the chelation of transition metal catalysts, and ROS detoxification by antioxidants [11]. Imbalances in ROS production and the activity of protection mechanisms can result in excessive direct exposure of cells to ROS, coupled with subsequent free radical-induced damage. These damaging effects of ROS are generally kept under control by endogenous antioxidant systems, which include glutathione, ascorbic acid, and enzymes such as superoxide dismutase, glutathione peroxidase, and catalase. Oxidative stress occurs when antioxidant systems are overwhelmed by ROS, and the resultant oxidative damage can lead to cell death. Neural stem/progenitor cells (NS/PCs) are known to be quite sensitive to increases in ROS and tend to result in cell apoptosis. Oxidative stress-induced apoptosis in NS/PCs has been frequently observed during NS cell therapy and therapeutic irradiation of the brain [12-14]. These findings indicate that oxidative damage to mitochondria is a pivotal event in oxidative cell damage, and mitochondrial ROS should be considered to be a primary target for drug development for the treatment of CNS disease [15, 16]. A number of proapoptotic and antiapoptotic proteins have been detected in the mitochondrial membrane. Cytochrome c, a component of the respiratory chain, has been identified as one of the proapoptotic molecules existing within the mitochondria [15]. The release of cytochrome c from the injured mitochondria was recently determined to activate caspase-3 [17]. Bcl-2 is an antiapoptotic protein, which is predominantly detected in mitochondria, and prevents the apoptosis induced by a variety of agents [18, 19]. Bcl-2 prevents cell death via the suppression of oxyradical-mediated membrane damage, the stabilization of mitochondrial membrane potential, and the prevention of cytochrome c release [20, 21].

Selenite, an essential dietary element for mammals, is detected in the active center of glutathione peroxidase(GPx), an antioxidant enzyme which protects membrane lipids and macromolecules against the oxidative damage generated by peroxides [22, 23]. Selenium is also required for the catalytic activity of mammalian thioredoxin reductase, another critical anti-oxidant enzyme [24, 25]. However, the antioxidant selenium (Se) has been identified as an essential micronutrient in mammals, and is present in the active center of GPx, an antioxidant enzyme which protects membrane lipids and macromolecules against oxidative damage caused by peroxides, including hydrogen peroxide [23]. Selenium is also a major component in the catalytic activation of another important antioxidant protein for mammals, thioredoxin reductase, and several other selenoproteins [25]. In addition, selenium has been determined to exert a protective effect against methamphetamine-induced neurotoxicity [26]. Moreover, the positive clinical responses observed during therapy with selenium and other antioxidants in neurodegenerative diseases have provided substantial evidence for the crucial role of free radicals and oxidative stress in pathologic processes [9]. The neuroprotective effects of Se have been reported at an experimental level in both methamphetamine- and 6- hydroxydopamine-induced toxicities [26], as well as in positive clinical responses during therapy with Se in neurodegenerative diseases [9].

In a previous report, we demonstrated some of the protective effects exerted by selenite on both neurochemical and behavioral markers of hydrogen peroxide (H_2O_2)-induced neurotoxicity in neural progenitor cells derived from rat spinal cord tissue. As these positive effects were related to the redox modulation evidenced by reduced lipid peroxidation, we therefore hypothesized

that such protective effects might directly involve its antioxidant properties, most probably associated with thioredoxin reductase expression, optimum H_2O_2 removal, and a consequent inhibition of proapoptotic events, including the activation of caspases 3 and 9. The present study was also conducted to investigate the effects of selenite on different markers of neurotoxicity and cell death induced by ROS following traumatic damage in rat spinal cord in *in vivo* approaches. For the *in vivo* experiments, the effects of selenite on H_2O_2 neurotoxicity were assessed using behavioral, biochemical, and morphological markers.

Materials and Methods

Adult spinal cord-derived neural progenitor cells culture

For preparation of adult spinal cord-derived NPCs, rats were anaesthetized deeply using a pentobarbital in 0.9% sterile saline solution and killed by decapitation. The region of the complete cervical enlargement (spinal cord level C3 through T1) was dissected out. After removal of the dura, the tissue was minced, washed in sterile Dulbecco's phosphate buffered saline (DPBS) and digested in a solution of 0.125% of trypsin, DNase (0.01%, Sigma) in Hank's balanced salt solution (HBSS) for 30min at 37°C. The cells were transferred to culture dishes containing serum free growth medium, which consists of NB medium with B27 supplement, bFGF (20ng/ml), and EGF (20ng/ml). Cells were either grown as neurospheres in petri dish, or poly D-lysine coated culture dish.

Sodium selenite treatment and H_2O_2 exposures

The cells were seeded in NB media for 8h. They were cultured in 5% O_2 in CO_2 incubator. Eighty percent density of cells were pretreated with sodium selenic acid (Na_2SeO_3) (10ng/ml) for 8h followed by H_2O_2 (0.3mM) for a further 6h. The optimum concentrations of selenite and H_2O_2 were selected according to the preliminary experiment related to cytotoxicity and survival effect of broad range of each reagent. Dilutions of H_2O_2 were made fresh from a 30% stock solution into Dulbecco's Modified Eagle's Medium (DMEM) just prior to each experiment. Exposures to H_2O_2 were performed by simple addition of a small volume of H_2O_2 diluted in DMEM at x 100 directly to each well, followed by light agitation. Cultures were incubated for the times noted and then toxicity or biochemical measurements were performed. We observed that the toxicity of H_2O_2 was reduced if the H_2O_2 exposures were not performed within 5min of dilution. This is likely due to the highly reactive nature of H_2O_2 and its short half-life in dilute solutions.

Analysis of cell viability

Cell viability was assessed by visual cell counts in conjunction with Tryphan Blue exclusion. Mitochondrial activity was assessed by measuring the ability of spinal cord-derived neural progenitor cells cultures to reduce MTT (3, 4, 5-dimethyl thiazol-2-yl) -2, 5-diphenyl tetrazolium bromide (MTT, Sigma) to a colored formazan using a plate reader. (Note; MTT is reduced to a colored insoluble formazan primarily by enzymes within the mitochondrial electron transport complex. Thus, the MTT assay is thought to represent a general measure of mitochondrial activity and therefore cellular oxidative capacity.) In all viability assays, triplicate wells were used for each condition, and each experiment was repeated at least three times.

Flow cytometry

Cells were cultured in 100mm dishes at densities that ensured exponential growth at the time of harvest. The harvesting and processing protocols used to detect DNA by flow cytometry with propidium iodide were done. Cells were analyzed with a BD Biosciences FACScan (San Jose, CA). Percentages of cells in the G0/G1, S, and G2/M stages of the cell cycle were determined with a DNA histogram fitting program (MODFIT; Verity Software, Topsham, ME). A minimum of 10^4 events/samples was collected.

RNA extraction and semi-quantitative RT-PCR (reverse transcription polymerase chain reaction)

Total cellular RNA was extracted with Trizol (Life Technologies, Frederick, MA), reverse transcribed into first strand cDNA using an oligo-dT primer amplified by 35 cycles (94ºC, 1min; 55ºC, 1min; 72ºC, 1min) of PCR using 20pM of specific primers. PCR amplification was performed using the primer sets. Duplicate PCR reactions were amplified using primer designed GAPDH as a control for assessing PCR efficiency and for subsequent analysis by 1.5% agarose gel electrophoresis. For labeling of PCR products, we used a Syber green detection kit which was purchased from Applied Biosystems (Foster, CA). Semi-quantitative RT-PCR was performed using an ABI7700 Prism Sequence Detection System. Primer sequences were designed using Primer Express software (PE-Applied Biosystems, Warrington, UK) using gene sequences obtained from the GeneBank database.

TUNEL and Caspases assays and quantification

The death of apoptotic cells after traumatic injury was estimated in terms of their ability to reduce the dye (3, 4, 5-dimethyl thiazol-2-yl) -2, 5-diphenyl tetrazolium bromide (MTT, Sigma) to blue purple formazan crystal. The effect of traumatic damage on the induction of apoptosis spinal cord tissue was determined with the TdT in situ apoptosis detector kit (Roche, USA), used according to the manufacturer's specifications. After fixation with 4% paraformaldehyde, H_2O_2- or selenite-pretreated NPC cells and injured tissue sections were incubated in TUNEL reaction mixture containing deoxynucleotidyl transferase (TdT) buffer with TdT and biotinylated dUTP, incubated in a humid atmosphere at 37°C for 90min, and then washed with PBS. The sections were incubated at room temperature for 30min with anti-horseradish peroxidase-conjugated antibody, and the signals were visualized with diaminobenzidine. The results were analyzed using a Fluorescence Microscope (Leica Microsystem, PA). TUNEL-positive apoptotic cells in SCI tissue lesion site were quantified

by counting of positively stained cells. Three digital microscopic images at a magnification of 100x were randomly captured at the areas where the positive cells were abundant around lesion site for each section. The number of positively stained cells in the three images was averaged. Three sections at each of the two sections were examined by an observer blind to the treatment and the mean value of cell counting was used to represent one single SCI tissue sample. The result was expressed as relative cells percentage per view field. The size of the view field was 0.075 mm^2. For Caspase-3, -8, and -9 activity assay, ten μg of protein in 50μl total volume was mixed with 50μl of equilibrated Caspase-Glo 3/7, 8, or 9 reagents (Promega). After incubating at room temperature for 1h, luminescence was measured using TD 20/20 Luminometer (Turner Designs, Sunnyvale, CA). Blank values were subtracted and fold-increase in activity was calculated based on activity measured from untreated cells. Each sample was measured in triplicate.

Measurement of intracellular ROS

Intracellular ROS was evaluated using the fluorescent probe DCFDA (5-(and-6)-carboxy-2', 7'-dichlorodihydro-fluorescein diacetate). For visualization by fluorescent microscopy, N_2A cells were plated in glass bottom dishes and treated with 0.3mM H_2O_2, alone or with selenite, for 6h. Cells were then washed and loaded with 10μM of DCFDA for 30min at 37°C, and imaged by fluorescent microscopy (ex/em=495/525nm). For quantitative assessment of ROS production, spinal cord-derived NPC cells in 96-well plates were washed with HBSS and loaded with 10μM of DCFDA for 30min at 37°C. Cells were washed three times with HBSS and exposed to 100μM of *t*BHP, alone or with SS-31. The oxidation of DCF was monitored in real time by a microplate spectrofluorometer (Molecular Devices, Sunnyvale, CA) using ex/em wavelengths of 485/530nm.

ATP measurement

The amount of protein was determined using the Protein Assay Kit (Bio-Rad, Hercules, CA, USA) following the manufacturer's instructions. Cells were resuspended in buffer containing 150mM/L KCl, 25mM/L Tris-HCl; pH 7.6, 2mM/L EDTA pH 7.4, 10mM/L KPO_4 pH 7.4, 0.1mM/L MgCl2 and 0.1% (w/v) BSA at a concentration of 1mg protein per ml of buffer. ATP synthesis was initiated by the addition of 250i l of the cell suspension to 750μl of substrate buffer (10mM/L malate, 10mM/L pyruvate, 1mM/L ADP, 40μg/ml digitonin and 0.15mM/L adenosine pentaphosphate). Cells were incubated at 37°C for 10min. At 0 and 10min, 50μl aliquots of the reaction mixture were withdrawn, quenched in 450μl of boiling 100mM/L Tris-HCl, 4mM/L EDTA pH 7.75 for 2min and further diluted 1/10 in the quenching buffer. The quantity of ATP was measured in a luminometer (Berthold, Detection Systems, Pforzheim, Germany) with the ATP Bioluminescence Assay Kit (Roche Diagnostics, Basel, Switzerland) following the manufacturer's instructions.

Western blot

For confirmation of differentially expressed proteins after selenite treatment in cultured NPC cells and injured spinal cords, dissected lesion site tissues from three or four injured or normal animals and selenite treated cells were pooled and homogenized (only tissue) and lysed in 500μl of lysis buffer (20mM Tris-HCl [pH 7.5], 150mM NaCl, 1mM EDTA, 1% Triton X-100, 2.5mM sodium pyrophosphate, 1mM EGTA, 1mM glycerophosphate, 1mM Na_3VO_4, and 1mM PMSF. Lysates were clarified by centrifugation at 15,000 x g for 10 min and the total protein content was determined by a Bio-Rad (Millan, Italy) protein assay kit. For western blotting, equal amounts (40μg) of protein extracts in a lysis buffer were subjected to 10% SDS-PAGE analysis and transferred to a nitrocellulose membrane. Anti-GFAP, anti-Nestin (1:500, Sigma), anti-MBP (1:400, Chemicon, USA), pSAPK/JNK (1:1000, Cell Signaling), anti-pERK (1:1000, Cell Signaling), anti-Bcl2 (1:1000, Cell Signaling), anti-Bax (1:1000, Cell Signaling), anti-P38 (1:1000, Cell Signaling), anti-Akt (1:1000, Cell Signaling), anti-Cytochrome c (1: 1000, Cell Signaling), and anti-β-Actin (1:500, Sigma) antibodies were incubated with membranes. Relative band intensities were determined by Quality-one 1-D analysis software (Bio-Rad, USA).

Animals and Spinal Cord Injury (SCI) induction and experimental design

Adult female Wistar rats weighting 260g or 6 weeks old rats were used in our experiments. Animal care was in compliance with Korean regulations on protection of animals used for experimental and other scientific purposes. Animals were subjected to a traumatic injury followed by modified protocol as described in detail in Kang *et al* [27]. Briefly, rats were anesthetized with ketamine (75mg/kg) and xylazine (10mg/kg). The spinous processes of T9 and T10 were removed with rongeurs and a laminectomy performed using a dental drill and rongeurs to expose the dorsal spinal cord. The dorsal and ventral columns, which include the dorsal and ventral corticospinal tract (CST), were cut by lowering microscissors attached to a sterotaxic arm to a depth of 3.5mm below the dorsal surface of the spinal cord and cutting twice. Experimental trials were first done to ascertain that this surgical procedure produced a consistent total transaction of the CST on both sides. For this study, we collected enough tissues those were timely harvested for biochemical examination. To evaluate the effect of selenite on acute phase SCI pathophysiology, we studied three group of rats ($n = 40$) with SCI by traumatic damage induction. The experimental groups was given selenite mixed with matrigel (Gibco-BRL) ($n = 30$) and the control group ($n = 10$, vehicle or matrigel only). To evaluate the effect of sodium selenite in pathogenic microenvironment of SCI (immediately after injury), the rats with SCI received varying concentrations of drugs (0, 10, 30, 50ng/kg) as treatment. Finally, we determined the optimum sodium selenite concentration was determined for effective treatment of SCI rats.

Sodium selenite administration

Various concentrations of purified sodium selenite were dissolved in HBSS, mixed according to the manufacture's instructions with matrigel (Gibco-BRL) (0, 10, 30, 50ng/kg) and injected directly into the lesion site immediately after injury. The control (vehicle) group received the same volume of DMSO mixed with matrigel only. The rats were randomly assigned into two groups: 30 SCI rats receiving the various concentrations

Fig. 1. Selenite reduced apoptotic cell death induced by hyperoxidation. (A) Cultured NPC cells were treated with several concentrations of H_2O_2 or selenite. (B, C) To demonstrate the effects of selenium on cell survival and proliferation, visual cell counts in conjunction with trypan blue exclusion methods and MTT (3, 4, 5-dimethyl thiazol-2-yl) -2, 5-diphenyl tetrazolium bromide (MTT, Sigma) assays were conducted. In all viability assays, triplicate wells were used for each condition, and each experiment was repeated at least three times. Raw data from each experiment were analyzed using analysis of variance with Fisher′ s or *t*-test (**P*<0.05, ***P*<0.01).

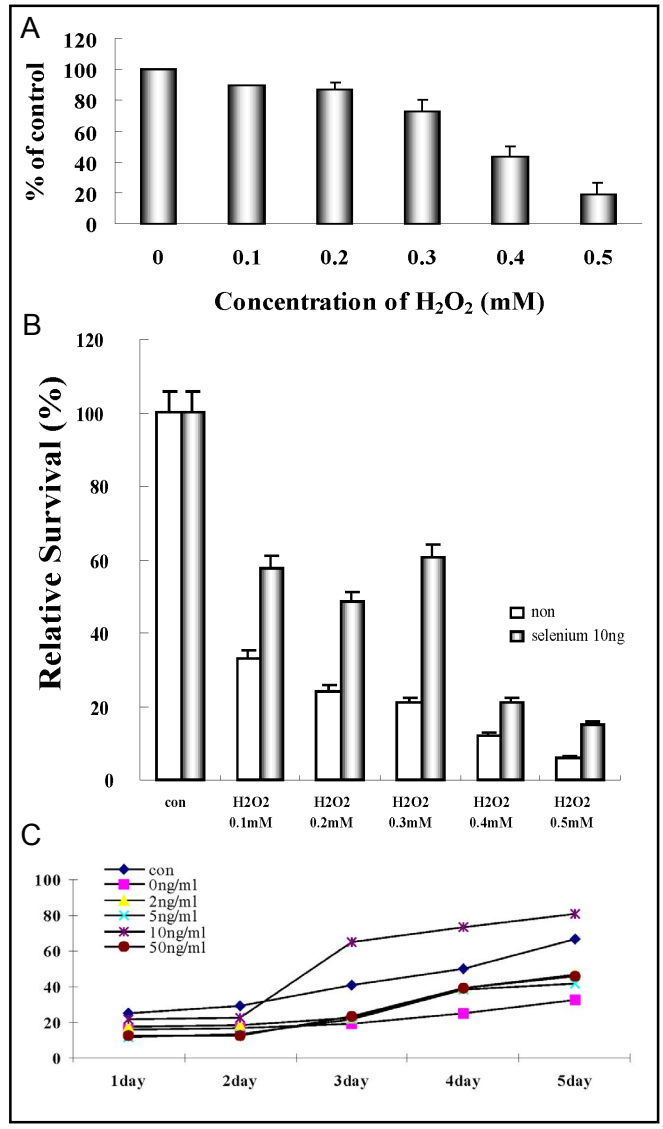

of the drug treatment and 10 SCI rats as control. A total of 40 animals were used in these experiments. Immediately after the spinal cord lesion, either the experimental treatment (selenite mixed with matrigel) or the control treatment (HBSS mixed with matrigel) were injected into the intrathecal space close to the T9-T10 lesion site of injured spinal cord. The skin incision was closed with silk sutures.

Histological analysis

The animals were sacrified under sodium pentobarbital anesthetized (60mg/kg, ip) and their spinal cord fixed by transcardial perfusion with 0.1M PBS followed by 4% paraformaldehyde in 0.1M phosphate buffer. Fixed spinal cord were equilibrated in 30% sucrose for 48 h and then cut into 10μm coronal sections on a frozen microtome. The intact control spinal cords and one sciatic nerve were also processed in the same manner. For analysis of protein upregulation in injured spinal cords, tissues at the center of the lesion were incubated with overnight at 4 °C with primary antibodies against anti-ED-1 (1:100, Serotec. UK) and anti-GFAP (1: 1500, DAKO Cytomation, Denmark). After extensive washing with PBS, the tissue sections were incubated for 30min with FITC, Texas–Red secondary antibodies (1: 250, Molecular Probe, USA). Cell nuclei were labeled with Topro-3 (Molecular Probe, USA). The results were analyzed using a Confocal Microscopy (Leica Microsystems, PA) using a Leica TCS sp2 laser scanning microscope equipped with 3 lasers. Immunohistochemical experiments were repeated at least three times. For Luxol Fast Blue (LFB) Staining, serial 10μm paraffin cross-sections of spinal cord 4 week post-injury control (HBSS injected) and selenite treated animal tissue sections were fixed and stained overnight at 60 °C in 0.1% Luxol Fast Blue (Sigma, Oakville, Ontario) in 95% ethanol, 0.5% acetic acid. In addition, counterstaining was carried out with 0.05% $LiCO_3$. Nerve cells staining were performed using 0.25% of Cresyl Echt Violet (Sigma). For each spinal cord segment, samples were harvested at 500μm intervals to yield 20 sections per spinal cord segment. Stained sections were viewed on an Olympus microscope (BH-2; Olympus, Melville, NY) at 40 x magnification and captured with a Magna Fire SP CCD camera (Optronics, Goleta, CA). Image capturing was done using Magna Fire SP 2.1 software (Optronics), and the image processing was done using Photoshop (Adobe). Stained sections around the injury epicenter were digitally imaged, and the area of Luxol Fast Blue staining was analyzed.

Functional recovery

Functional tests were performed after administration of selenite or control HBSS. Animals were placed on a restricted diet to motivate them to perform the various behavioral tests. Behavioral recovery was scored according to the BBB (Basso, Beattie, Bresnahan) scale, which is composed of 21 different criteria of the movement of the hind limb from complete paralysis to complete mobility. BBB score 0 represents no hindlimb movement and 20 represents normal mobility. Statistical analysis was carried out using the statview software package (SAS, Cary, NC).

Statistical analysis

All data were presented as mean ± SEM from five or more independent experiments. The statistical significance of difference between groups was calculated by using the Student's two tailed *t*-test.

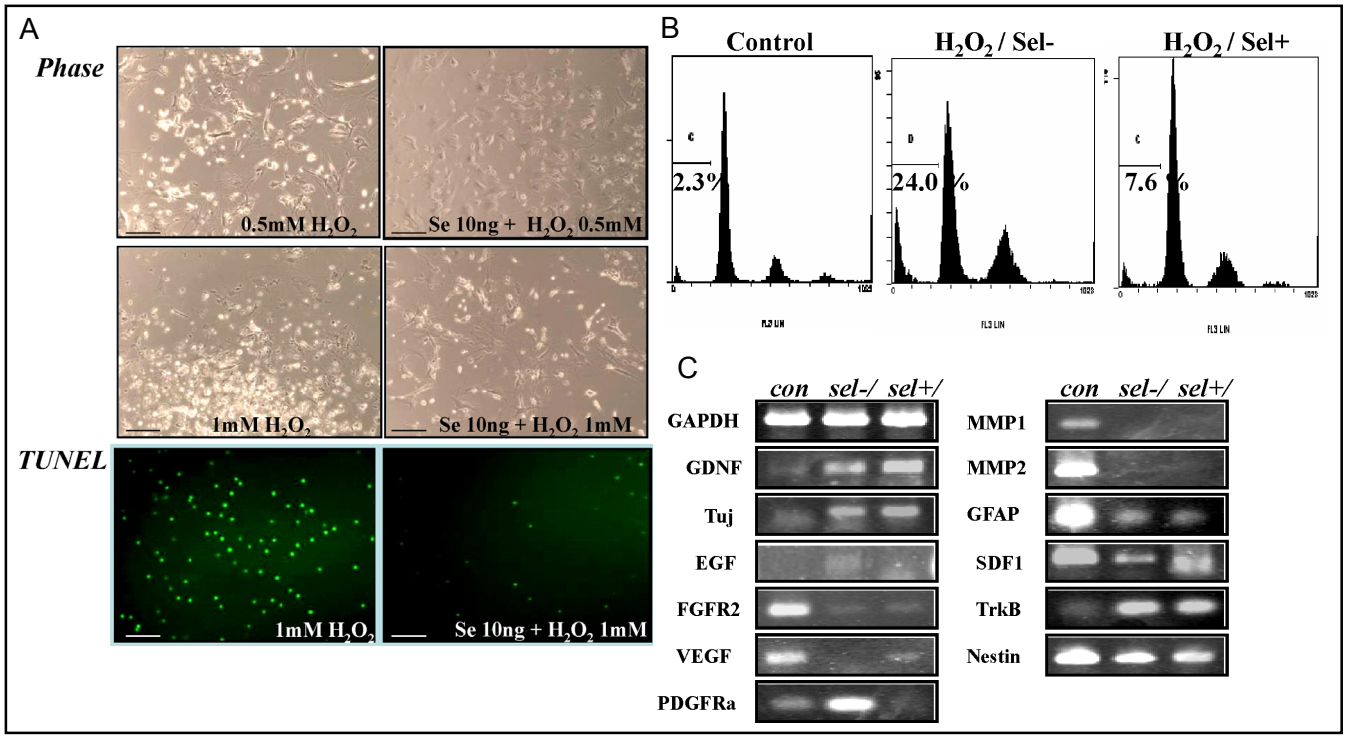

Fig. 2. Selenite reduced apoptotic cell death and induced differential gene expression. Cultured NPC cells were treated with several concentration of H_2O_2 alone or with selenite pretreatment (10ng/ml). (A) Cell viability was assessed via TUNEL staining. TUNEL- positive apoptotic cells were quantified via the counting of the positively stained cells. *Bars*, 20 μm. (B) Cells were cultured in 100mm dishes at densities that ensured exponential growth at the time of harvest. The harvesting and processing protocols used to detect DNA by flow cytometry with propidium iodide were conducted. The cells were analyzed with a BD Biosciences FACScan (San Jose, CA). The percentages of cells in the G0/G1, S, and G2/M stages of the cell cycle were determined using a DNA histogram fitting program (MODFIT; Verity Software, Topsham, ME). A minimum of 104 events/sample was collected. (C) The effects of selenite on the genetic expression of NPC cells via semi-quantitative RT-PCR. Total cellular RNA was extracted with Trizol (Life Technologies, Frederick, MA), reverse transcribed into first strand cDNA using an oligo-dT primer amplified by 35 cycles (94 °C, 1min; 55 °C, 1min; 72 °C, 1min) of PCR using 20pM of specific primers. PCR amplification was performed using the primer sets. Duplicate PCR reactions were amplified using designed GAPDH primer as a control for the evaluation of PCR efficiency.

Results

Sodium selenite protects neural progenitor cell from H_2O_2-induced apoptotic cell death and affected cell growth

H_2O_2-induced cell death was apparent in the two day culture of neural progenitor cells, but was not observed in selenium-pretreated cultures at a concentration of 10ng/ml (Fig. 1A, 2A). 60% of the neural progenitor cells were shown to have survived in the 10ng/ml selenite-pretreated culture after treatment with 0.3mM H_2O_2 (Fig. 1B). Cultured neural progenitor cells were capable of growth in a selenium containing medium at a concentration of 10ng/ml after treatment with 0.3mM H_2O_2 (Fig. 1C). Neural progenitor cells grew well from the 2nd to 5th days of the experimental period with 10ng/ml selenite pretreatment being the optimal concentration.

Effect of selenite on gene expression of neural precursor cells after H_2O_2 treatment

Selenite exerted prominent effects on the expression of various functional genes, including several types of matrix metalloproteinases (MMPs), and stem cell markers by neural progenitor cells cultured in the presence or absence of selenium prior to H_2O_2 treatment. Selenium did not significantly alter the basal mRNA levels of GDNF, Nestin, SDF1, or TrkB, whereas it reduced the quantity of GFAP and PDGFR*a* at a concentration of 10ng/ml (Fig. 2C).

Sodium selenite induced cell protection against H_2O_2-mediated cell death via modulation of P38, JNK, Bax, Bcl-2 expression in vitro and in vivo

Cell survival requires the active inhibition of apoptosis, which is accomplished either by the inhibition

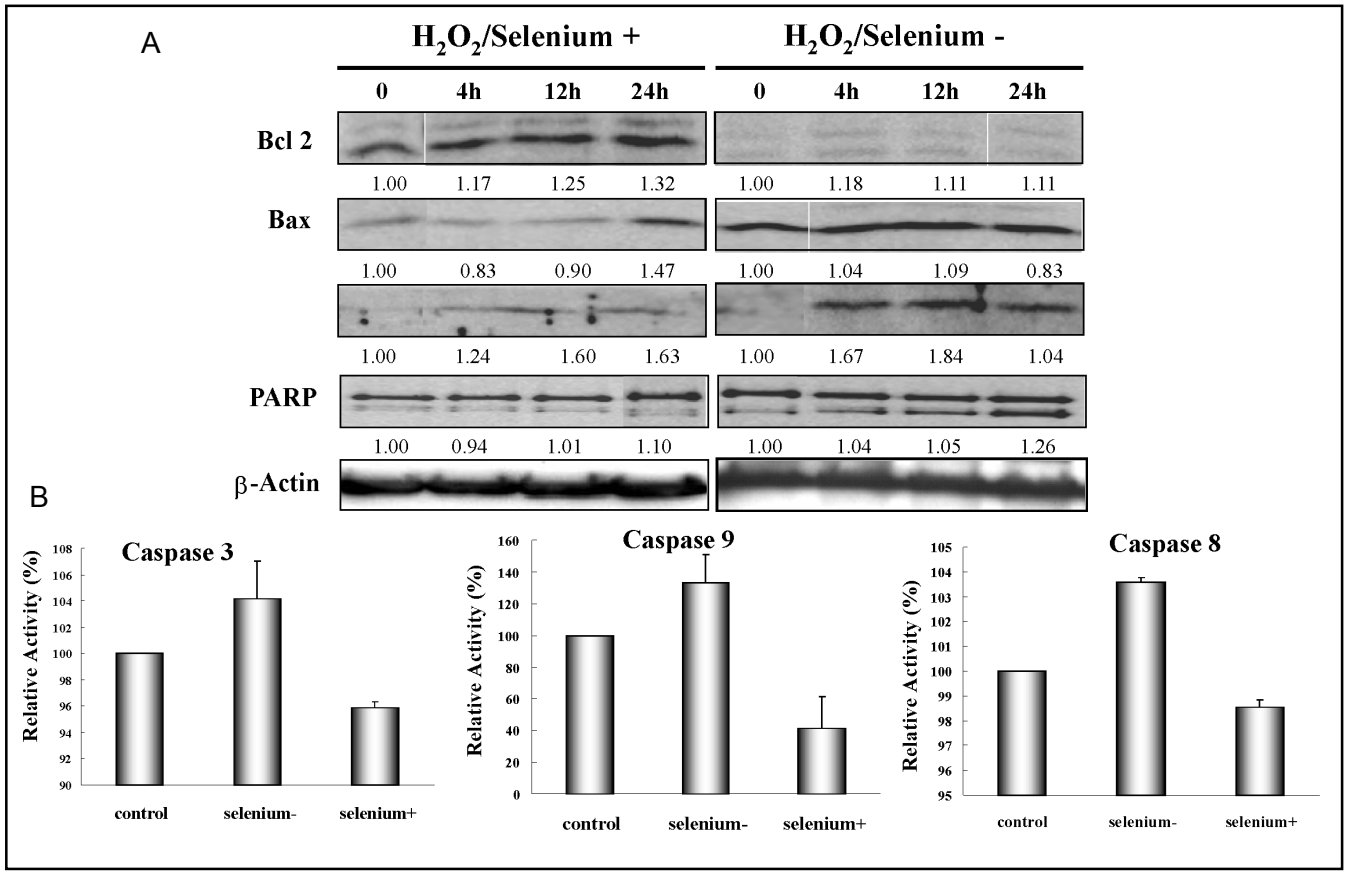

Fig. 3. Differential expression of the signal proteins in the cultured NPC cells after selenite treatment. For the confirmation of differentially expressed apoptotic signal proteins after selenite treatment, the cells were pooled and lysed in 500µl of lysis buffer. The lysates were clarified via centrifugation at 15,000 x g for 10 min, and the total protein contents were assessed using a Bio-Rad (Millan, Italy) protein assay kit. (A) For western blotting, equal amounts (40µg) of protein extracts in lysis buffer were subjected to 10% SDS-PAGE analysis and transferred to nitrocellulose membranes. Relative band intensities were determined by Quality-one 1-D analysis software. Each sample was measured in triplicate. (B) For Caspase-3, -8, and -9 activity assay, 10 ug of protein in a 50µl total volume was mixed with 50µl of equilibrated Caspase-Glo 3/7, 8, or 9 reagents (Promega). After incubating at room temperature for 1h, luminescence was measured using a TD 20/20 Luminometer (Turner Designs, Sunnyvale, CA). Blank values were subtracted and fold-increase in activity was calculated based on activity measured from untreated cells. Each sample was measured in triplicate. Raw data from each experiment were analyzed using analysis of variance with Fisher′s or t-test (**P*<0.05, ***P*<0.01).

of enhanced cell death via the blockage of DNA breakage (Fig. 2B) or the activation of their functional proteins for survival. Survival and proliferation factors induced the activation of p-Akt, p-ERK1/2, and Bcl-2 upregulation in the selenite-pretreated cultures. The selenite treated cells also evidenced attenuated p-SAPK/JNK, Bax, Cytochrome c, and PARP activation. In particular, selenite attenuated the activation of mitochondrially mediated cell death-related proteins via the modulation of caspase 3 and 8 activity, and cytochrome C release (Fig. 3).

In order to determine the *in vivo* neuroprotective functions of selenite, we utilized a rat spinal cord injury model. One week after injury, the group of selenite-treated animals evidenced an induction of Bcl2 and Bcl xl after one week of spinal cord injury (Fig. 7). Damage to the spinal cord also causes an extensive proliferation of cells in and around the epicenter, many of which are microglia and macrophages (Fig. 6). In the selenite-treated animal groups, we noted more or less decreased infiltration and activation of ED-1 positive cells (Fig. 6). However, p38 and p-SAPK/JNK signaling proteins evidenced slightly decreased or profoundly increased levels of TuJ, Bcl 2, and thioredoxin reductase (TR1) in the selenite-treated animals (Fig. 7). Our results indicated that selenite prominently attenuated mitochondrially-mediated cell death signal pathways and ultimately negatively regulated neuronal cell death in injured spinal cord tissues.

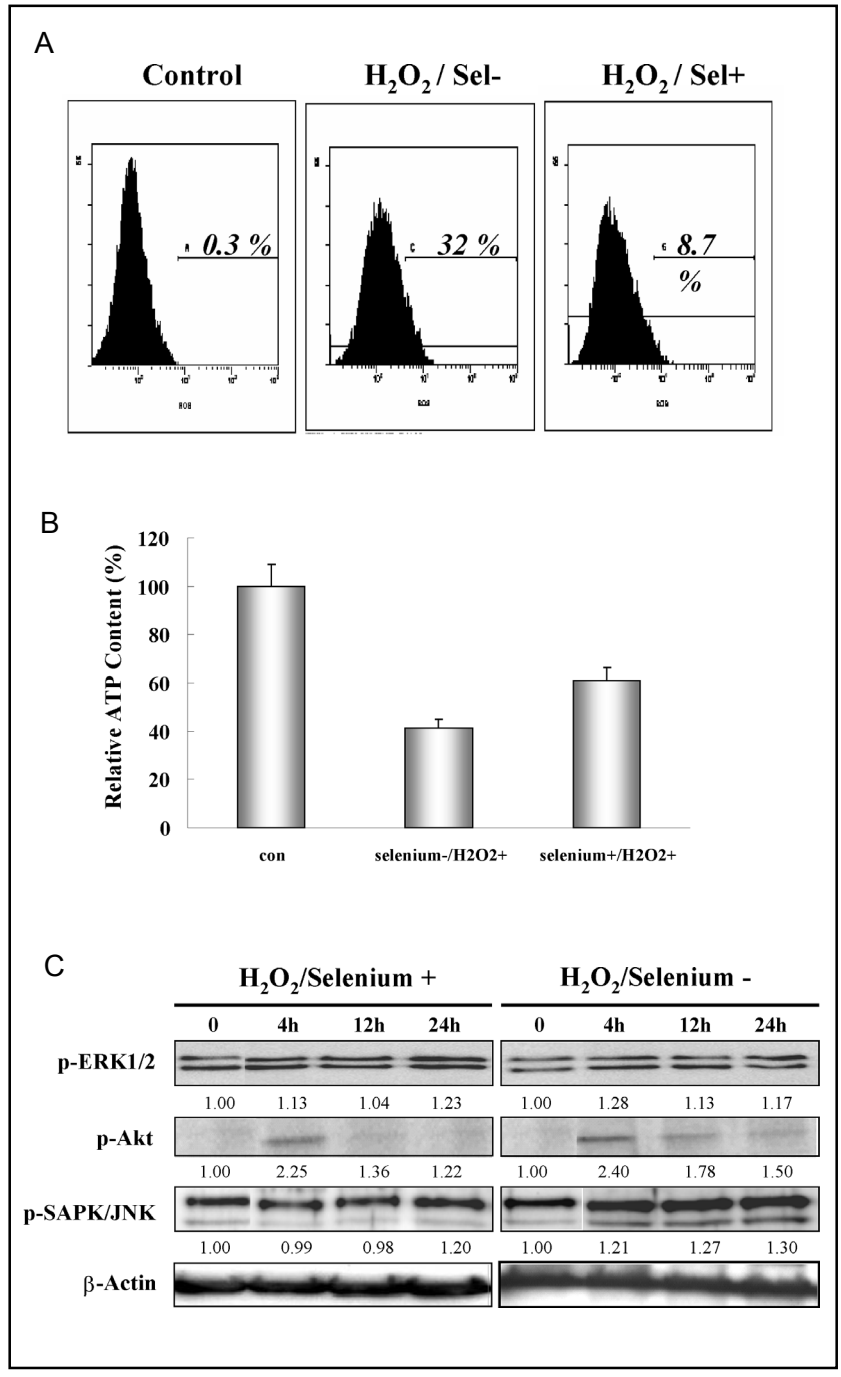

Fig. 4. Effects of selenite on H_2O_2-induced apoptotic features in cultured neural progenitor cells. (A) Intracellular ROS was evaluated using the fluorescent probe DCFDA (5-(and-6)-carboxy-2', 7'-dichlorodihydrofluorescein diacetate). For visualization by fluorescent microscopy, NPC cells were plated in glass-bottomed dishes and treated with 50iM *t*BHP, alone or with SS-31, for 6h. The cells were then washed and loaded with 10 μM of DCFDA for 30min at 37°C, and imaged by fluorescent microscopy (ex/em=495/525nm). For quantitative assessments of ROS production, NPC cells in 6-well plates were washed with HBSS and loaded with 10μM of DCFDA for 30 min at 37°C. The cells were washed three times with HBSS and exposed to 0.3mM of H_2O_2, either alone or with selenite (100nM). DCF oxidation was monitored in real time with a microplate spectrofluorometer (Molecular Devices, Sunnyvale, CA) using ex/em wavelengths of 485/530nm. (B) ATP synthesis was initiated by the addition of 250μl of the cell suspension to 750μl of substrate buffer. The cells were incubated for 10 minutes at 37°C. At 0 and 10min, 50μl aliquots of the reaction mixture were withdrawn, quenched in 450μl of boiling 100mM/L Tris-HCl, 4 mM/L EDTA pH 7.75 for 2min and further diluted to 1/10 in the quenching buffer. The quantity of ATP was measured in a luminometer with the ATP Bioluminescence Assay Kit in accordance with the manufacturer's instructions. Raw data from each experiment were analyzed via analysis of variance with Fisher's or *t*-test (**P*<0.05). (C) For confirmation of differentially expressed apoptotic signal proteins after selenite treatment, cells were pooled and lysed in 500μl of lysis buffer. Lysates were clarified by centrifugation at 15,000 x g for 10min and the total protein content was determined by a Bio-Rad (Millan, Italy) protein assay kit. For western blotting, equal amounts (40μg) of protein extracts in a lysis buffer were subjected to 10% SDS-PAGE analysis and transferred to a nitrocellulose membrane. Relative band intensities were determined by Quality-one 1-D analysis software. Each sample was measured in triplicate.

Sodium selenite inhibit H_2O_2-induced apoptotic features in cultured neural progenitor cells

Hydrogen peroxide (H_2O_2) has been implicated in increases in cellular oxidative stress. We evaluated the effects of selenite on ROS production after H_2O_2 treatment in cultured neural progenitor cells. Hydrogen peroxide increased DCF oxidation in a concentration-dependent manner, and the increased DCF fluorescence intensity was abolished by 10ng/ml of sodium selenite (Fig. 4A). Selenite itself did not alter the production of ROS, but selenite reduced H_2O_2-induced ROS production from 32% to 8.7% (Fig. 4A). We also attempted to determine whether selenite could inhibit the release of cytochrome C from the mitochondria in the selenite-treated cells. The results of Western blot analysis indicated that while the H_2O_2-treated cells released a great deal of their

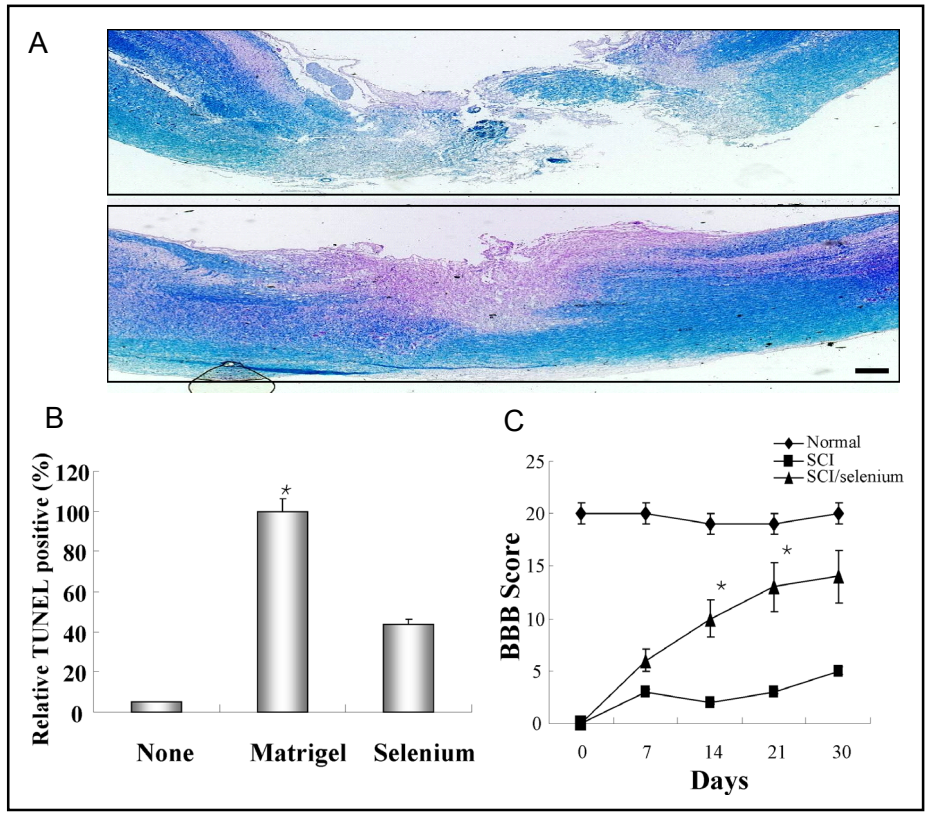

Fig. 5. The effects of selenite on the alleviation of demyelination and apoptotic cell death in the injured spinal cords. The attenuation of demyelination and apoptotic cell death after traumatic damage to the spinal cord. (A) Representative micrographs at the injury lesions from normal and injured animals stained respectively with Cresyl Echt Violet and Luxol Fast Blue. Traumatic injury induces demyelination and neuron degeneration in the spinal cord. Nerve cell staining was conducted with 0.25% Cresyl Echt Violet solution. *Bars*, 50 μm. (B) The effects of selenite on traumatic damage inducing apoptosis in spinal cord tissue was determined with the TdT *in situ* apoptosis detection kit, used in accordance with the manufacturer's specifications. The results were analyzed via Fluorescence microscopy (Leica Microsystem, PA). TUNEL- positive apoptotic cells in SCI tissue lesion sites were quantified by counting the positively stained cells. (C) Locomotor recovery after treatment of selenite in SCI rats. Repeated ANOVAs showed that the BBB scores differed significantly between the groups, and also changed significantly over the survival time. The BBB scores in selenium-injected animals were significantly higher than those of the SCI control rats. After 3 days, the selenite-injected animals evidenced gradual improvement through week 4. **P*<0.05 using the one way ANOVA test. The values were expressed as the means ± SEM. of ten animals per group. Statistical analysis was performed using repeated ANOVAs. The arrowhead on the abscissa indicates the time of selenite treatment. Data were expressed as the mean ± SD (n = 40). **P*<0.05 using the Student's two tailed *t*-test.

cytochrome c into the cytosol, cells preincubated with selenite reduced cytochrome c release into the cytosol (Fig. 3A), thereby indicating that selenite prevents H_2O_2-induced cell death via the maintenance of mitochondrial integrity. As H_2O_2 triggers caspase activation, we also attempted to determine whether selenite can inhibit caspase 3, caspase 8, and caspase 9 activation in H_2O_2-treated NPC cells. In response to H_2O_2 exposure, caspase3 activity increased by approximately 1.5-fold, but selenite treatment induced a significant blockage of H_2O_2-elicited caspase activation (Fig. 3B). We also evaluated the ATP production functions of selenite/ H_2O_2-treated cells. In response to H_2O_2 exposure, ATP production was prominently reduced, but selenium pretreatment significantly recovered the ATP production ability of cells (Fig. 4B). Together, these findings showed that selenite inhibits H_2O_2-induced apoptotic features in spinal cord-derived neural progenitor cells.

Sodium selenite attenuated apoptotic cell death in lesion site of spinal cord

Traumatic injuries to the spinal cord resulted in cell death. After or prior to the administration of selenite mixed with matrigel into the lesion site, injury-induced cell death was demonstrated via TUNEL staining. Few TUNEL-positive cells were observed in the lesion site one week after traumatic injury. Selenite treatment effectively prevented the injury-induced TUNEL positive cells (Fig. 5B). The results of Western blot analysis revealed negligible PARP, Bax, and Bcl2 expression in the cytosolic compartment of the non-injured normal spinal cord tissue sampled from equivalent spinal segments (T9-T11) (Fig. 7). In the SCI rats, PARP expression was detected at significant levels (Fig. 7). Selenite-treated animals evidenced sharp reductions in the apoptotic signal protein, PARP, and Bax, and prominent increases in the Bcl2 survival protein.

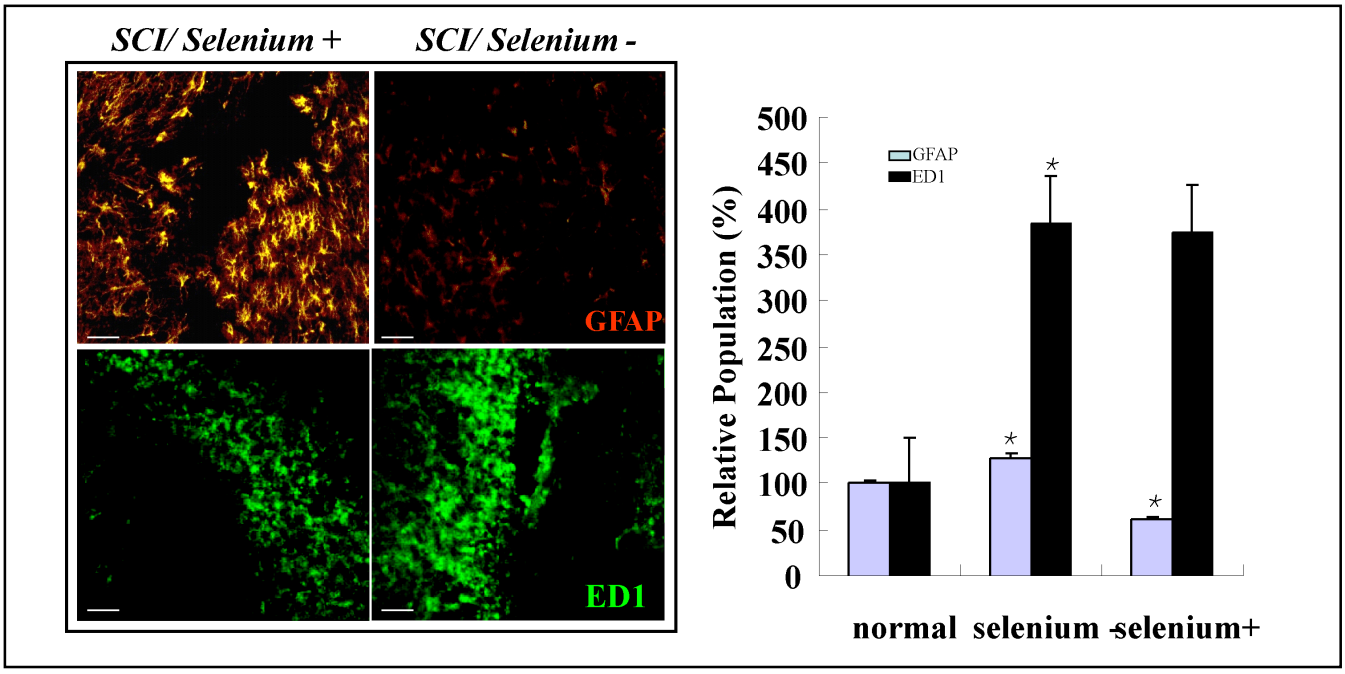

Fig. 6. Immunostaining with anti-ED-1 and GFAP antibodies at the lesion site of injured spinal cord. One week after injury, ED-1 antigen expression increased slightly in selenite-treated SCI animals as compared with the untreated control SCI animals. Normal rat spinal cord tissue does not express ED-1 antigens. For analysis of astrogliogenesis and microglia and macrophage activation after selenite treatment in injured spinal cords, tissues at the center of the lesion were incubated with primary antibodies against anti-GFAP (1:1500) and anti-ED-1 (1:100). After extensive washing with PBS, these tissue sections were incubated for 30 minutes with FITC and Texas–Red secondary antibodies (1:250). Cell nuclei were labeled with Topo-3 (Molecular Probe, USA). The results were analyzed using Confocal Microscopy. The number of GFAP-positive glias was compared between the two experimental groups (*P<0.05). *Bars*, 40 µm.

Selenite attenuated injury induced astrogliosis, hypomyelination, and neuron cell death

In an effort to determine whether selenite inhibited posttraumatic astrogliosis, the number of GFAP-positive glia in the two experimental groups were compared. Spinal cord sections obtained 3mm caudal to the injury epicenter were examined quantitatively for GFAP-positive glial cells in the ventral funiculi, a region of white matter containing axonal tracts, which is important for rat locomotion. As a result, 5.0 ± 2.0 astroglia were detected per 20ìm of tissue in the selenite-treated group vs 33.0 ± 1.9 astroglia per 20ìm of tissue in the control SCI group (Fig. 6). The number of GFAP-immunopositive cells in the ventral funiculi evidenced an overall significant effect on the reduction of reactive astrogliosis (Fig. 6). In contrast to the GFAP-positive population, we noted considerably more TuJ-positive neuron cells surrounding the lesion site (data not showed).

Myelin and neuronal staining were detected in the lesion sites of the spinal cord epicenter (Fig. 5A). In normal spinal cords and selenite-treated rats, light blue myelin and violet wave cell groups indicated myelination and the prevention of neuronal death. By way of contrast, in the SCI control group in the same area, very weak LFB staining and Cresyl Echt Violet staining were detected. Selenite treatment improved significantly in the LBF positive region and increased MBP expression was observed around the lesion site in the selenite/SCI administrated group, which indicated that hypomyelination occurred after the insult (Fig. 5A). Selenite treatment also reduced the loss of neurons in the epicenter area of the spinal cord. Cresyl Echt Violet staining in the lesion epicenter of the SCI control tissue completely disappeared, whereas this loss was not observed in the normal and selenite-treated animals (Fig. 5A). Finally, selenite treatment reduced and attenuated demyelination and neuronal death in the lesion sites. The overall cross-section profiles of the lesion epicenters from the normal control, matrigel/SCI, and selenite/SCI animals were comparable. In an attempt to determine whether selenite treatment reduced lesion volume, we outlined the lesion area in transverse sections of the spinal cord sample from the injury epicenter, as well as adjacent tissue up to 5mm rostral and caudal to the epicenter. Measurements of the

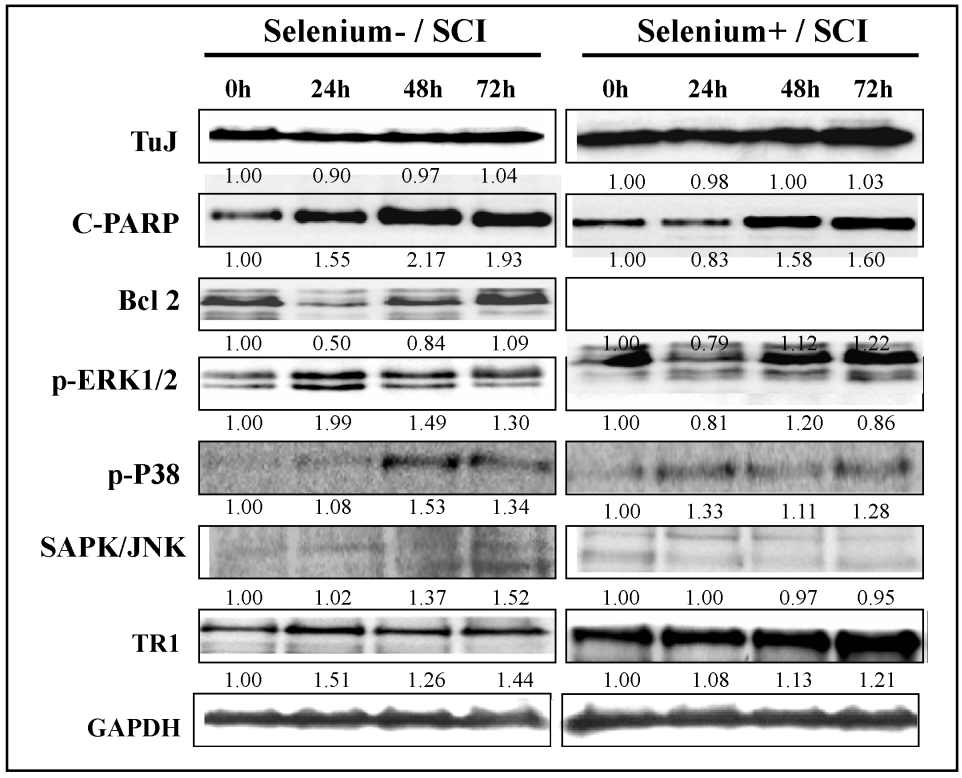

Fig. 7. Differential expressions of the apoptotic signal proteins in the lesion site after selenite treatment. For confirmation of differentially expressed signal proteins and neuron marker (TuJ) after selenite treatment, tissues at the center of the lesion were isolated from the traumatic injured spinal cord and were isolated and analyzed. Relative band intensities were determined by Quality-one 1-D analysis software.

longitudinal and transverse lesion lengths also indicates the significant effects of selenite. The gray matter track of the lesion site may have been influenced by possible neuroprotective properties possessed by the selenite.

We observed a dose dependent effect of selenite at several concentrations (0, 10, 30, 50μg/kg) on Caspase 3, 8, 9, and PARP expression by containing TUNEL positive cells at the injury epicenter. Selenite at 10μg/kg showed significant blocking effect essentially reducing Caspases and PARP expression to negligible pre-SCI levels (data not showed).

Functional recovery

In order to determine whether selenite may protect against traumatic damage, including secondary motor neuronal damage in SCI, the rats were treated with selenite immediately after injury, and their recovery of motor function was evaluated for 30 days using a modified Basso, Beattie, and Bresnahan (BBB) hind limb locomotor rating scale (Fig. 5C). Although motor function was only impaired slightly in the control/SCI rats, the animals undergoing SCI evidenced extensive deficits in hind limb movement. In the first three days following the administration of SCI, we noted no differences in the extent of locomotor dysfunction between the selenite-treated and control SCI groups of rats, thereby showing that all animals experienced the same degree of injury. However, by the fifth day post-injury, motor recovery was significantly improved in the selenite-treated animals, and they continued to regain motor function, whereas no such effects were observed in the SCI control group. 10 days post-injury and treatment, the selenite-treated rats were able to slightly support their weight, whereas the control SCI animals evidenced only limited joint experiments (Fig. 5C).

Effect of selenite on macrophage and microglia infiltration and activation in spinal cord injury rat model

Sham operated or control SCI animals and selenite-treated (10μg/kg) animals were evaluated after 1 week of surgery and treatment. We noted no statistical differences between the control and experimental group in terms of the number of ED-1 immunopositive cells in all segments during the examination period. The expression of ED-1 antigenic protein level and ED-1 immunopositive cells were slightly increased following selenite treatment (Fig. 6). Selenite treatment exerted no direct effects on macrophage invasion. Few ED-1 immunopositive cells were observed within the normal tissue (Fig. 6). Seven days after the administration of selenium and the placebo, slightly enlarged ED-1 immunopositive cells were detected within the lesion sites. Traumatic injury stimulated the activation of macrophages and microglia in the lesion site,

as was shown by the results of ED-1 immunohistochemistry. The number of activated macrophages was significantly increased. They evidenced a dark staining with round sharp and blunt processes of the lesion site tissue one week after injury (Fig. 6).

Discussion

Oxidative stress and the generation of reactive oxygen species (ROS) have been confidently implicated in a number of neuronal and neuromuscular disorders, including stroke and cerebrovascular disease, Alzheimer's disease, Parkinson's disease, familial amyotrophic lateral sclerosis, and Duchenne's muscular dystrophy [28-34]. Selenium has been shown to provide protection against ROS-induced cell damage, and the proposed mechanisms principally invoke the functions of GPxs and selenoprotein P (SelP). Selenium/selenite has been associated with regulatory functions in cell growth, survival, cytotoxicity, and transformation, possibly involving redox regulation and chemical toxicity, as well as the regulation of the transcription of various genes [25]. The precise biochemical activities of selenite, however, remain to be fully resolved. Thioredoxin reductase and thioredoxin form a redox system that performs multiple roles, including the redox regulation of transcription factors and the provision of reducing equivalents for deoxyribonucleotide synthesis, a precursor to DNA synthesis. Selenium induces the mitochondrial permeability transition via the modification of protein thiol groups, which induces cytochrome c release and a loss of mitochondrial membrane potential [35]. Here, we provide experimental support for the hypothesis that selenite may perform a pivotal function in anti-oxidation responses, in part via the significant inhibition of the production of ROS, an important mediator in the pathophysiology of inflammatory disease, including acute spinal cord injury. The activation of both resident and recruited immune cells appears to be the cellular source for the upregulation of these cytokine mRNA in SCI-induced CNS inflammation [3]. Macrophages perform important functions in the removal of myelin debris and the products of neuronal degeneration following trauma, infection, or autoimmune reactions within the neuronal systems.

An important intracellular signal transduction pathway which results in apoptosis after spinal cord injury involves caspase activation. Recent evidence [3] suggests that this activation may be responsible for the apoptosis induced by proinflammatory cytokines. It is apparent that the inflammatory responses of LPS in macrophages include the initial induction of ROS in macrophages, which results in the activation of MAPKs and NFκB and to the induction of iNOS and inflammatory cytokines. This final step would result in NO production in toxic quantities, together with toxic cytokines. Selenite can alleviate these effects via antioxidant activity and via the modulation of the downstream pathway. Our results show that the selenite-modulated pathway is p38/JNK and PARP, Bax, and cytochrome c specific. ERK evidenced little involvement in these processes. The short-term effect of selenite is principally anti-apoptotic. Cellular damage from ROS was significantly alleviated. Selenite incubation induced a reduction in the intracellular ROS levels, and the prevention of p38, SAPK-JNK, and Bax activation in *in vitro* cultures. Caspase activations were also effectively prevented (Fig. 3B). The activation of the caspase 3 pathway occurs following spinal cord injury at the trauma site. The present study extends these observations to the epicenter of SCI by providing the first evidence to demonstrate that an upregulation of the PARP and Bcl2 proteins also perform an important function in the execution of apoptosis in the injured spinal cord. The activated caspase-3 protease contributes to the execution of apoptosis via PARP. In addition, the cleavage of the DNA repair enzyme of PARP during apoptosis not only blocks attempts at DNA repair, but also preserves the cellular pools of ATP that may be necessary for the execution of the cell death program. Compared with the SCI control animals, the tissue lesions in selenite-treated SCI animals evidenced profound reductions in PARP apoptotic proteins and increases in the expression of Bcl2, the anti-apoptotic survival protein (Fig. 7). Oligodendrocyte apoptosis is a widely dispersed phenomenon occurring during SCI, which results in long-term and persistent demyelination. As each oligodendrocyte myelinates multiple axons, their death results in the denouement of many fibers that remained intact after the initial trauma. Selenite attenuated apoptotic cell death, including PARP activity, reduced astrogliogenesis, and hypomyelination, phenomena which occur in areas of active cell death in injured spinal cords (Fig. 5, 6) and can interfere with protein function. Therefore, it may also negatively influence cell metabolism and survival. PARP activity is generally thought to contribute to neuronal cell death under a variety of neurological conditions [36], including traumatic brain injury [37, 38] and SCI [39], as a consequence of energy failure or via the modification of the activity of various proteins by poly (ADP-ribosylation) [40]. Selenite effectively blocks PARP-mediated

apoptotic cell death in lesion sites (Fig. 7). The principal protective effect of selenite in SCI would therefore be manifested in the suppression of acute secondary apoptotic cell death. Indeed, selenite treatment prevented the elevation of myelin levels and a neuron protein (TuJ) detected in the spinal cords of SCI rats, but it does not appear to attenuate active microglia and macrophage infiltration (Fig. 6 and 7). This finding supported the lack of histopathological changes observed in the lesion areas of selenite-treated SCI rats (Fig. 5). Moreover, selenite-mediated neuroprotection has been linked to the selenite-induced attenuation of the p38 mitogen-activated protein kinase, pSAPK/JNK (Fig. 7).

Our results show that selenite administered immediately after SCI significantly diminishes the apoptotic cell death caused by SCI, and also reduces functional deficits. The selenite-treated group recovered hind limb reflexes more rapidly, and a higher percentage regained responses similar to those of the non-injured rats. The treated rats also proved to more effectively regain the coordinated use of their hindlimbs to allow for the maintenance of their downward-oriented position on an inclined plane (Fig. 5C). The overall functional improvement, measured in terms of hindlimb use as assessed by the BBB scale, was found to be significantly enhanced in the selenium-treated group as compared to the SCI control rats (Fig. 7). Our data indicated that the therapeutic outcome of selenite treatment was most likely attributable to its comprehensive prevention of apoptotic cell death, thus protecting the white matter, oligodendrocytes, and neurons, as well as inhibiting astrogliosis. The hindlimb deficits in this lower thoracic SCI model were found to be attributable largely to the loss of white matter axonal tracts [41, 42]. To a considerably lesser degree, the death of motor neurons associated with trunk stability [43] is an additional contributing factor. Selenite functions via the inhibition of the processes of apoptotic cell death in the lesion sites of the spinal cord, and has been suggested as an agent that might be responsible for delayed cell death in white matter pathology (Fig. 5A and 5B). Selenite significantly attenuated white matter damage and enhanced ventral horn motor neuron survival at spinal cord levels adjacent to the lesion site (Fig. 4). More importantly, the profound correlation between white matter preservation and enhanced motor function recovery further corroborates the hypothesis that selenite treatment facilitated the recovery of hindlimb function in the SCI model via the reduction of later-phase white matter loss, which contributes significantly to the deleterious consequences associated with SCI. Moreover, we noted a discernable reduction in the number of reactive astrogliosis in the spared white matter (Fig. 6). Reactive astrocytes secrete inhibitory molecules including neurocan and trabecular meshwork-inducible glucocorticoid response protein (TIGR) to restrict motor neuronal repair and regeneration [44, 45]. In addition, astroglial scarring prevents axonal regeneration [45].

The contribution of selenite to the reduction of apoptotic cell death and the prevention of myelin destruction in white matter stimulated by traumatic injury requires further study, in order to elucidate the operant mechanisms. The finding that selenite prevents secondary pathological events in traumatically injured spinal cords and promotes the recovery of motor functions in an animal model may facilitate the development of novel drug targets for the treatment of SCI.

Acknowledgements

This work was supported by the 21st Century Frontier/ Stem Cell Research Committee (SC3130) in South Korea.

References

1 David S, Aguayo AJ: Axonal elongation into peripheral nervous system "bride" after central nervous system injury in adult rats. Science 1981;214:931-933.

2 Taoka Y, Okajima K, Uchiba M, Murakami K, Kushimoto S, Johno M, Naruo M, Okabe H, Takatsuki K: Role of neutrophils in spinal cord injury in the rat. Neuroscience 1997;79:1177-1182.

3 Carlson SL, Parrish ME, Springer JE, Doty K, Dossett L: Acute inflammatory response in spinal cord following impact injury. Exp. Neuro. 1998;151:77-88.

4 Richardson SJ: Free radical in the generation of Alzheimer's disease. Ann N Y Acad Sci 1993;67:119-127.

5 Olanow CW: An introduction to the free radical hypothesis in Parkinson's disease. Ann Neurol 1992:S2-9.

6 Olanow CW: A radical hypothesis for neurodegeneration Trends Neurosci 1997;16:439-444.

7 Bellavite P: The superoxide-forming enzymatic system of phagocytes. Free Radical Biol Med 1988;4:225-261.

8 Giulian D, Vaca K, Corpuz M: Brain glia release factors with opposing actions upon neuronal survival. J Neurosci 1993;13:29-37.
9 Halliwell B, Gutteridge JM: Biologically relevant metal ion-dependent hydroxyl radical generation: an update. Fedn Eur Biochem Socs Lett 1992;307:108-112.
10 Richter C, Kass GE: Oxidative stress in mitochondria: its relationship to cellular Ca2+ homeostasis, cell death, proliferation, and differentiation. Chem Biol Interact 1991;77:1-23.
11 Yu BP: Cellular defenses against damage from reactive oxygen species. Physiol Rev 1994;74:139-162.
12 Limke TL, Rao MS: Neural stem cell therapy in the aging brain: pitfalls and possibilities. J Hematother Stem Cell Res 2000;12:615-623.
13 Le Belle JE, Svendsen CN: Stem cells for neurodegenerative disorders: where can we go from here? BioDrugs 2002;16:389-401.
14 Limoli CL, Giedzinski E, Rola R, Otsuka S, Palmer TD, Fike JR: Radiation response of neural precursor cells: linking cellular sensitivity to cell cycle checkpoint, apoptosis and oxidative stress Radiat Res 2004;161:17-27.
15 Liu X, Kim CN, Yang Y, Jemmerson R, Wang X: Induction of apoptosis program in cell-free extracts: requirement for dATP and cytochrome c. Cell 1996:86;145-157.
16 Murphy MP, Smith RA: Drug delivery to mitochondria: the key to mitochondrial medicine. Adv Drug Deliv Rev 2000;41:235-250.
17 Kluck RM, Bossy-Wetzel E, Green DR, Newmeywer DD: The release of cytochrome c from mitochodria: a primary site for Bcl-2 regulation of apoptosis. Science 1997;275:1132-1136.
18 Itoh NM, Tsujimoto Y, Nagata S: Effect of Bcl-2 on Fas antigen-mediated cell death. J Immunol 1993;151:621-627.
19 Reed JC: Double identity for proteins of the Bcl-2 family. Nature 1997;387:773-776.
20 Bruce-Keller AJ, Begley JG, Fu W, Butterfield DA, Bredesen DE, Hutchins JB, Hensley K, Mattson MP: Bcl-2 protects isolated plasma and mitochondrial membranes against lipid peroxidation induced by hydrogen peroxide and amyloid B-peptide. J Neurochem 1998;70:31-39.
21 Desagher S, Martinou JC: Mitochondria as the central control point of apoptosis. Trends Cell Biol 2000;10:369-377.
22 Rotruck JT, Pope AL, Ganther HE, Swanson AB, Hafeman DG, Hoekstra WG: Selenium: biochemical role as a component of glutathione peroxidase. Science 1973;179:588-590.
23 Harman D: Free radicals and age-related disease, in Free Radicals in Aging 1993:pp.205-222.
24 Marcocci L, Floche L, Packer L: Evidence for a functional role of the selenocysteine residue in mammalian thioredoxin reductase. Biofactors 1997;6:351-358.
25 Lee SR, Bar-Noy S, Kwon S, Levine RL, Stadtman TC, Rhee SG: Mammalian thioredoxin reductase: oxidation of the C-terminal cysteine/selenocysteine active site forms a thioselenide, and replacement of selenium with sulfur markedly reduces catalytic activity. roc Natl Acad Sci USA 2000;97:2521-2526.
26 Imam SZ, Newport GD, Islam F, Slikker W, Jr Ali SF: Selenium, an antioxidant, ptotects against methamphetamine-induced dopaminergic neurotoxicity. Brain Res 1999;818:575-578.
27 Kang SK, So HH, Moon YS, Kim CH: Proteomic analysis of injured spinal cord tissue proteins using 2DE and MALDI-TOF. Proteomics 2006;6(9):2797-2812.
28 Dexter DT, Carter CJ, Wells FR, Javoy-Agid Y, Lees A, Jenner P, Marsden CD: Basal lipid peroxidation in substantia nigra is increased in Parkinson's disease. J Neurochem 1989;52:381-389.
29 Smith CD, Carney JM, Starke-Reed PE, Oliver CN, Stadtman ER, Floyd RA, Markesbery WR: Excess brain protein oxidation and enzyme dysfunction in normal aging and Alzheimer disease. Proc Nat Acad Sci USA 1991;88:10540-10543.
30 Tan S, Wood M, Maher P: Oxidative stress induces a form of programmed cell death with characteristics of both apoptosis and necrosis in neuronal cells. J Neurochem 1995;71:95-105.
31 Ragusa RJ, Chow CK, Porter JD: Oxidative stress as a potential pathogenic mechanism in an animal model of Duchenne muscular dystrophy. Neuromuscul. Disord 1997;7:379-386.
32 Cornett CR, Markesbery WR, Ehmann WD: Imbalances of the trace elements related to oxidative damage in Alzheimer disease brain. Neurotoxicology 1998;19:339-345.
33 Facchinetti F, Dawson VL, Dawson TM: Free radicals as mediators of neuronal injury. Cell Mol Neurobiol 1998;18:667-682.
34 Sagara Y, Tan S, Maher P, Schubert D: Mechanisms of resistance to oxidative stress in Alzheimer's disease brain. Neurotoxicology 1998;19:339-345.
35 Kim TS, Jeong DW, Yun BY, Kim IY: Dysfunction of rat liver mitochondria by selenite: induction of mitochondrial permeability transition through thiol-oxidation. Biochem Biophys Res Commun 2002;294:1130-1137.
36 Skaper SD: Poly (ADP-Ribose) polymerase-1 in acute neuronal death and inflammation: a strategy for neuroprotection. Ann NY Acad Sci 2003;993:217-228.
37 Whalen MJ, ClarkRS, Dixon CE, Robichaud P, Marion DW, Vagni V, Graham S, Virag L, Hasko G, Stachlewitz R: Traumatic brain injury in mice deficient in poly-ADP (ribose) polymerase: a preliminary report. Acta Neurochir Suppl 2000;76:61-64.
38 LaPlac MC, Zhang J, Raghupathi R, Li JH, Smith F, Bareyre FM, Snyder SH, Graham DI, McIntosh TK: Pharmacologic inhibition of poly (ADP-ribose) polymerase is neuroprotective following traumatic brain injury in rats. J Neurotrauma 2001;18:369-376.
39 Scott GS, Jakeman LB, Stokes BT, Szabo C: Peroxynitrite production and activation of poly (adenosine diphosphate-ribose) synthetase in spinal cord injury. Ann Neurol 1999;45:120-124.
40 Burkle A: Physiology and pathophysiology of poly(ADP-ribosyl)ation. BioEssays 2001;23:795-806.
41 Blight AR: Cellular morphology of chronic spinal cord injury in the cat: analysis of myelinated axons by line-sampling. Neurosci 1983;10:521-543.
42 Teng YD, Choi H, Onario RC, Zhu S, Desilets FC, Lan S, Woodard EJ, Snyder EY, Eichler ME, Friedlander RM: Minocycline inhibits contusion-triggered mitochondrial cytochrome c release and mitigates functional deficits after spinal cord injury. PNAS 2004;101:3071-3076.
43 Holstege G: Descending motor pathways and the spinal motor system: limbic and non-limbic components. Prog Brain Res 1991;87:307-421.
44 Jones LL, Margolis RU, Tuszynski MH: The chondroitin sulfate proteoglycans neurocan, brevican, phosphacan, and versican are differentially regulated following spinal cord injury. Exp Neurol 2003;182:399-411.
45 Jurynec MJ, Riley CP, Gupta DK, Nguyen TD, McKeon RJ, Buck CR: TIGR is upregulated in the chronic glial scar in response to central nervous system injury and inhibits neurite outgrowth. Mol Cell Neurosci 2003;23:69-80.